*8th International Conference on
the Stability of Ships and Ocean Vehicles*
Escuela Técnica Superior de Ingenieros Navales

111

LASHING OF TRAILERS ON – BOARD RO/RO SHIPS UNDER INTENSIVE ROLLING

N. Themelis & K.J. Spyrou,
School of Naval Architecture & Marine Engineering
National Technical University of Athens (Greece)

Abstract

We are analysing the lashing of trailers on board a RO/RO ferry from the perspectives of legislative requirements, ship and trailer motion dynamics and lashings' structural strength. We present a mathematical model giving the lashing loads for a trailer placed on the vehicle deck while the ship is performing rolling motion in beam waves. Furthermore we are presenting a finite element approach for determining the stresses that are developed at the lashing points on the trailer. The longer term objective is to produce an integrated model with enough detail that can be used for examining the reliability of a lashing system under realistic conditions

.

1. INTRODUCTION

Inappropriate securing of trailers and of other heavy vehicles on board RO/RO ships can cause human injuries, cargo damage, and in some extreme cases it could put in danger even the safety of the ship as a whole. Trailer lashings' arrangement and type should be suitably designed and attached so that, with an acceptable probability of exceedance, the loads produced due to ship motions (primarily rolling and to a lesser extent pitching) do not reach the prescribed limiting value representing lashings' strength.

International as well as national organisations (e.g. IMO [1-6], ISO [7-8], MCA [9]) have published guidelines concerning the efficient securing and stowage of cargo transported by sea. In particular, several Administrations require availability on board of an approved Cargo Securing Manual (CSM) as defined by IMO for all ships engaged in the carriage of non-bulk (solid or liquid) cargo [5], [10]. In conjunction with this, simplified procedures for calculating the maximum securing loads have been developed. These procedures rely on the anticipated accelerations at various locations of vehicle deck(s), taking into account the speed, the length and the beam to metacentric height ratio of the ship. Nonetheless, the true dynamics of a lashed trailer, which cannot always be assumed as rigidly attached to the deck, is not part of the calculation process. There have been a few attempts to improve on this by developing modelling approaches from first principles: Andersson [11] and Turnbull & Dawson [12-13], were the first who modelled the dynamics of a trailer with torsionally rigid or flexible chassis assuming sinusoidal-type ship motion (with maximum amplitudes for roll respectively 30^0 and 20^0 and for pitch 8^0 and 5^0). The experienced loads on the lashings are determined by solving the trailer motion equations and then their maximum values are checked if they exceed lashing strength. In MCA's Code of Practice [9] (developed on the basis of the work of Turnbull & Dawson), the

8th International Conference on
the Stability of Ships and Ocean Vehicles
Escuela Técnica Superior de Ingenieros Navales

112

maximum allowable load on a lashing was 95 kN [12]. According to the CSM, lashings' strength should be measured on the basis of the *maximum securing load* (MSL) which, for chains is 50% of the breaking strength and for re-usable wire ropes 30% [10].

A modelling approach integrating ship motions in waves, trailer dynamics and lashings' strength analysis appears as the natural next step of a "first principles" approach. Working towards this direction, certain improvements are discussed in the present paper: these are, the linking of the wave environment with the loads experienced on the lashings and the assessment of strength at critical locations on the basis of a finite element method, taking into account also dynamic loads.

2. CALCULATION OF LOADS IN THE CARGO SECURING MANUAL

On the trailer are acting inertial forces due to the longitudinal, transverse and vertical accelerations of the adjacent vehicle deck. The values assumed in the CSM are shown in Table 1. These values are corrected for deviations of ship length, speed and B/GM from their reference values which are, respectively, 100m, 15 knots and 13, assuming operation during the whole year and duration of voyage 25 days (!). The correction factors are given in the Tables 2 and 3.

The adequacy of the securing device is checked by considering the static balance of forces and moments in three circumstances featuring transverse sliding, transverse tipping and longitudinal sliding. These can be prevented if the sum of lashing loads (corresponding to their calculated strength) plus the friction are greater than the external loads.

From the above it is apparent that the time-dependent character of lashing loads, and thus the dynamic nature of the problem, is neglected. In fact, it is not possible to deduce

the safety margin for given weather conditions since such a connection to the environment is missing. Furthermore, characteristics of the trailer, e.g. those concerning the trestle and the suspension, are not considered. As a result, the lashings appear bearing the same load, which is not particularly realistic.

In Figs. 1, 2 and 3 are shown the effects of trailer's longitudinal and vertical position, ship speed, B/GM and MSL on lashings' safety margin, taking into account sliding and tipping in the transverse direction (these correspond to the rolling condition that will be considered later).

Table 1

	Transverse acceleration a_y (m/sec²)											Long. acc. a_x (m/sec²)
Upper Deck	7.1	7.1	6.9	6.8	6.7	6.7	6.8	6.9	7.1	7.4	7.4	3.8
Main Deck	6.5	6.5	6.3	6.1	6.1	6.1	6.1	6.3	6.5	6.7	6.7	2.9
Lower Deck	5.9	5.9	5.6	5.5	5.4	5.4	5.5	5.6	5.9	6.2	6.2	2.0
Tank Top	5.5	5.5	5.3	5.1	5.0	5.0	5.1	5.3	5.5	5.9	5.9	1.5
L(m)	0	0.1	0.2	0.3	0.4	0.5	0.6	0.7	0.8	0.9	1	L(m)
Vertical acceleration a_z (m/sec²)												
	7.6	7.6	6.2	5.0	4.3	4.3	5.0	6.2	7.6	9.2	9.2	

Table 2

Speed (kn)	Ship length (m)										
	50	60	70	80	90	100	120	140	160	180	200
9	1.20	1.09	1.00	0.92	0.85	0.79	0,7	0.63	0.57	0.53	0.49
12	1.34	1.22	1.12	1.03	0.95	0.90	0,79	0.72	0.65	0.60	0.56
15	1.49	1.36	1.24	1.15	1.07	1.00	0.89	0.80	0.73	0.68	0.63
18	1.64	1.49	1.37	1.27	1.18	1.10	0.98	0.89	0.82	0.76	0.71
21	1.78	1.62	1.49	1.38	1.29	1.21	1.08	0.98	0.90	0.83	0.78
24	1.93	1.76	1.62	1.50	1.40	1.31	1.17	1.07	0.98	0.91	0.85
27	2.08	1.90	1.75	1.62	1.51	1.41	1.27	1.16	1.06	0.99	0.92
30	2.23	2.04	1.88	1.74	1.62	1.51	1.37	1.25	1.14	1.07	0.99

Table 3

Deck	B/GM						
	7	8	9	10	11	12	13 or above
Upper Deck	1.56	1.40	1.27	1.19	1.11	1.05	1.0
Main Deck	1.42	1.30	1.21	1.14	1.09	1.04	1.0
Tween Deck	1.26	1.19	1.14	1.09	1.06	1.0	1.0
Lower Deck	1.15	1.12	1.09	1.06	1.04	1.02	1.0

8th International Conference on
the Stability of Ships and Ocean Vehicles
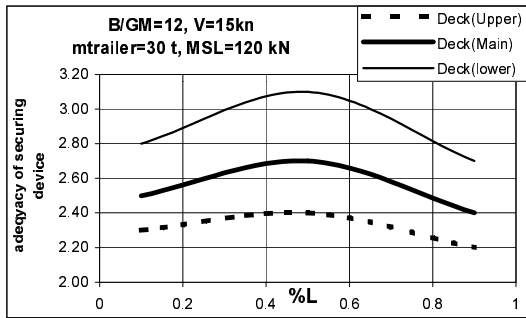*Escuela Técnica Superior de Ingenieros Navales*

113

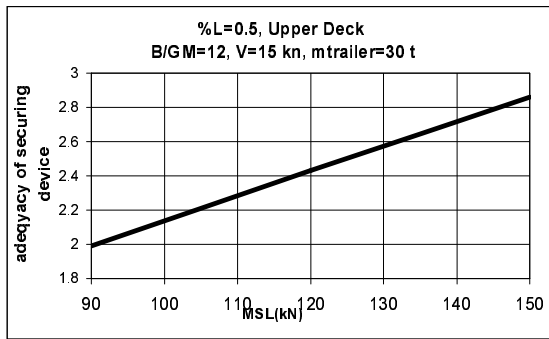Fig. 1: Effect of trailer's position on safety margin

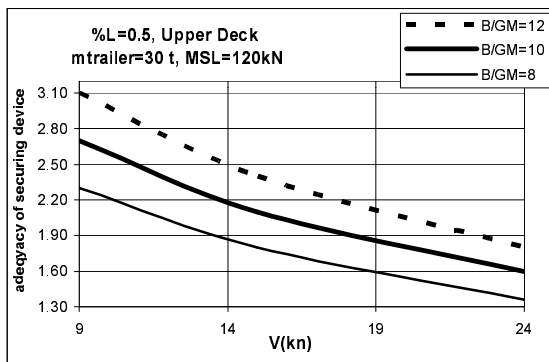Fig. 2: Effect of the assumed MSL value.

Fig. 3: Effect of speed and of the B/GM ratio.

3. THE TRAILER –LASHING SYSTEM

The main objective of our modelling process is the calculation of the forces that the lashings should bear in order to restrain the motion of the trailer relatively to the deck. As a first step we are examining only transverse motion caused by beam-sea rolling. Following in principle the approach of Turnbull & Dawson [12-13] we are modelling the trailer on the basis of point masses connected to a spine while the lashings are modelled by linear springs. The detailed form of the equations that govern the dynamics of each component of the trailer-lashings system are described in the next sub-sections.

3.1. Trailer

A typical trailer with its lashings is shown in Fig. 4.
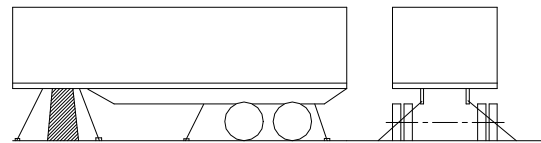
Fig. 4: Typical trailer - lashing arrangement.

In our model the trailer has a spine that is torsionally flexible in the longitudinal direction but rigid in bending. The mass of the trailer is distributed by six point masses. Fig. 5 shows the modelling of the trailer.
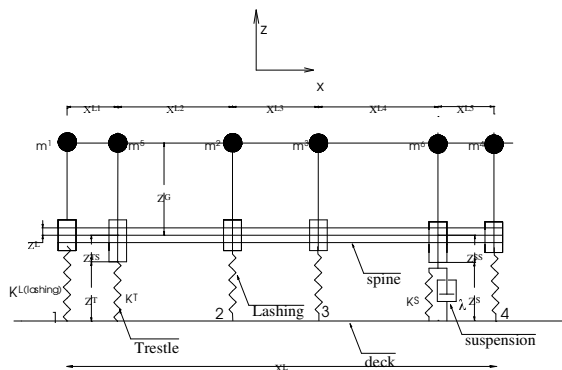

Fig. 5: Simplified model of the trailer

As shown in Fig. 5, we placed one point mass above the trestle, one at the suspension and one

*8th International Conference on
the Stability of Ships and Ocean Vehicles
Escuela Técnica Superior de Ingenieros Navales*

114

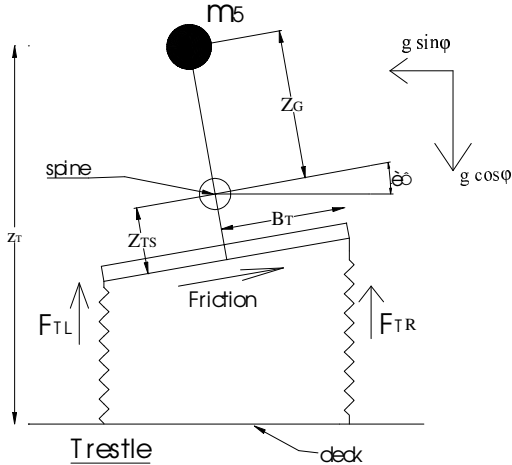at each spar. The trestle supports the trailer and the suspension is assumed to coincide with the

Fig. 6: Model of the trestle

position of the wheels. The spars contain the points where the lashings are connected to the spine. Also, they are rigid and they can rotate independently about the centre of the spine. As we examine only the relative motion of the trailer due to pure ship rolling, each lashing lies on a vertical plane that is perpendicular to the spine. As a matter of fact, the motion of each mass should be described by its vertical, z and transverse, y, displacements as well as by the angle of rotation θ. With three degrees of freedom for each mass, in the present analysis the trailer is modelled to have finally eighteen degrees of freedom.

3.2. Trestle

The trestle is usually constructed by steel and it could be modelled by two parallel connected linear springs (Fig. 6). As mentioned earlier, the longitudinal motion of the masses is neglected. The angle φ is the roll angle of the ship (and thus of the deck where the trailer is located) with respect to an earth fixed system (absolute angle).

The vertical forces of the two springs of the trestle, left and right hand side are due to the law of Hook for linear springs:

$$F = K * x \qquad (1)$$

where K, x are the stiffness of the spring and its instantaneous displacement, respectively. According to Fig. 6, the forces on the left and right side of the trestle are:

$$F_{TL,R} = K_T[z_T - (Z_G + Z_T)\cos\theta_T \pm B_T \sin\theta_T - Z_T] \quad (2)$$

The plus sign is for the force acting at the right side. All symbols are explained in the Nomenclature near the end of the paper. The total force acting on trailer due to the trestle is:

$$F_T = F_{TL} + F_{TR} \qquad (3)$$

3.3. Suspension

The suspension is modelled as a pair of springs with dampers (Fig. 7). The force at each side of the suspension due to the parallel connection of the spring and the damper is of the type
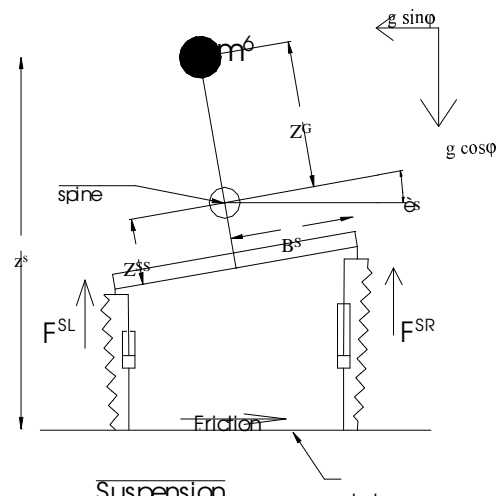

Fig. 7: Model of the suspension

*8th International Conference on
the Stability of Ships and Ocean Vehicles
Escuela Técnica Superior de Ingenieros Navales*

115

$$F = K * x + \lambda * \dot{x} \qquad (4)$$

where λ is the damping coefficient. Therefore, according to Fig. 7 the left and right suspension forces are:

$$F_{SL,R} = K_S[z_S - (Z_G + Z_{SS})\cos\theta_S \, \mu B_S \sin\theta_S - Z_S]$$
$$+ \lambda\{\dot{z}_S + \dot{\theta}_S[(Z_G + Z_{SS})\sin\theta_S \, \mu B_S \cos\theta_S]\} \qquad (5)$$

The plus signs correspond to the right force. The total force due to the suspension is:

$$F_S = F_{SL} + F_{SR} \qquad (6)$$

3.4. Lashing spars

The spars protrude from the spine and are the points where the lashings are attached to the trailer. The lashings are modelled by linear springs, so the load carried by a lashing is of the type:

$$F = (L - L_0)K \qquad (7)$$

where L, L_0 and K are respectively, the instantaneous length of the spring, the initial length, and the stiffness of the lashing. The length L_{Li} of the left lashing i is:

$$L_{Li} = \sqrt{S_{Li}^2 + T_{Li}^2} \qquad (8)$$

where S_{Li}, T_{Li} are the transverse and vertical component of L_{Li}. They are expressed according to Fig. 8 as follows:
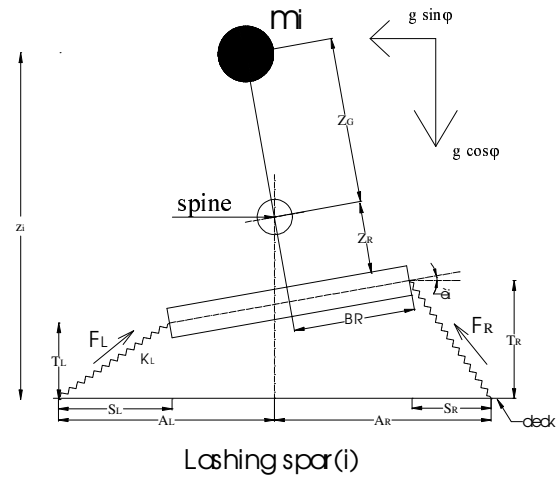

Fig. 8: Model at the lashing spar *i*.

$$S_{Li} = A_{Li} + y_i + Z_{Li}\sin\theta_i - B_{Li}\cos\theta_i \qquad (9)$$

$$T_{Li} = z_i - Z_G\cos\theta_i - Z_{Li}\cos\theta_i - B_{Li}\sin\theta_i \qquad (10)$$

According to equation (7), the total load on the left lashing at position *i* is:

$$F_{Li} = (L_{Li} - L_{0i})K_{Li} \qquad (11)$$

We have made the assumption that the lashings should be pre-tensioned. Thus, their length L cannot be less than the initial length L_0. The assumption is:

$$L \geq L_0 \qquad (12)$$

The total load on the left lashing *i* has a vertical and transverse component, which are:

$$F_{LZi} = F_{Li} * T_{Li} / L_{Li} \qquad (13)$$

$$F_{LYi} = F_{Li} * S_{Li} / L_{Li} \qquad (14)$$

The equations for the lashing on the right side can be developed in a similar way.

*8th International Conference on
the Stability of Ships and Ocean Vehicles
Escuela Técnica Superior de Ingenieros Navales*

116

4. EQUATIONS OF MOTION

4.1. Ship rolling

Ship rolling incurs inertial forces on the trailer which can be calculated by solving the following well-known differential equation of rolling motion according to an inertial coordinate system:

$$(I + \delta I)\ddot{\varphi} + B(\dot{\varphi}) + R(\varphi) = F_w(t) \qquad (15)$$

where φ is the absolute roll angle, $B(\dot{\varphi})$ is the damping moment, $R(\varphi)$ is the restoring and $F_w(t)$ is the wave moment which in this analysis is based on the Froude-Krylov assumption. We consider that the ship is excited by long beam waves. Also:

$$B(\dot{\varphi}) = B_e \dot{\varphi} \qquad (16)$$
$$R(\varphi) = \Delta * GZ(\varphi) \qquad (17)$$
$$GZ(\varphi) = GM\varphi + a_3\varphi^3 + a_5\varphi^5 + ... + a_9\varphi^9 \quad (18)$$
$$\omega_o = \sqrt{\frac{\Delta.GM}{I + \delta I}}$$
$$(19)$$

According to Fig. 9 the total transverse and vertical force (with reference to the deck) have components of the tangential force T, the centrifugal C and the gravity force mg. They are calculated as follows [17]:
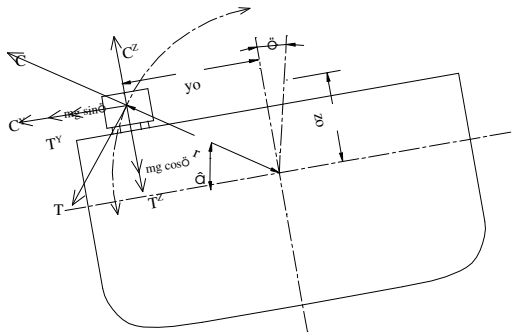

Fig. 9: Forces due to rolling, where m is the mass of the cargo unit.

$$R_Y = -mg * \sin\varphi - T_Y - C_Y \qquad (20)$$
$$R_Z = mg * \cos\varphi + T_Z - C_Z \qquad (21)$$
$$T_Y = mr.\sin\beta.\ddot{\varphi} \qquad (22)$$
$$T_Z = mr.\cos\beta.\ddot{\varphi} \qquad (23)$$
$$C_Y = mr.\cos\beta.\dot{\varphi}^2 \qquad (24)$$
$$C_Z = mr.\sin\beta.\dot{\varphi}^2 \qquad (25)$$

By solving (15) and inserting $\dot{\varphi}$, $\ddot{\varphi}$ into (20)-(25) we can determine the excitation incurred on the trailer due to the rolling of the ship. As a result the trailer will tend to move against the deck where it is lashed on.

4.2. Motion of the mass at the trestle

According to Fig.6, the equation of motion of mass 5 in the direction vertically to the deck is:

$$m_5 * \ddot{z} = R_{Z5} - F_T \qquad (26)$$

Similarly, along the deck the equation is:

$$m_5 * \ddot{y} = R_{Y5} - F_T * \mu_T * sign(\dot{y}_T) \qquad (27)$$

Taking moments about the centre of the mass m_5 of the trestle forces, the friction and considering also the spine torsion we obtain:

$$\begin{aligned}I_5 * \ddot{\theta}_T = &-F_{TR}[(Z_G + Z_{TS})\sin\theta_T + B_T * \cos\theta_T] + \\ &+F_{TL}[-(Z_G + Z_{TS})\sin\theta_T + B_T * \cos\theta_T] - \\ &- F_T * \mu_T(Z_G + Z_{TS})sign(\dot{y}_T) - \\ &-S_{K1}(\theta_T - \theta_1) - S_{K2}(\theta_T - \theta_2)\end{aligned} \qquad (28)$$

where S_{K1}, S_{K2} are respectively the torsional stiffness of the spine between the trestle - lashing 1 and trestle – lashing 2.

4.3. Suspension

The equations of motion of mass 6 are (Fig. 7):

*8th International Conference on
the Stability of Ships and Ocean Vehicles
Escuela Técnica Superior de Ingenieros Navales*

117

$$m_6 * \ddot{x} = R_{Z6} - F_S \qquad (29)$$

$$m_6 * \ddot{y} = R_{Y6} - F_S * \mu_S * sign(\dot{x}) \qquad (30)$$

$$I_6 * \ddot{\theta}_S = -F_{SR}[(Z_G + Z_{SS})\sin\theta_S + B_S * \cos\theta_S] +$$
$$+F_{SL}[-(Z_G + Z_{SS})\sin\theta_S + B_S * \cos\theta_S] -$$
$$-F_S * \mu_T * z_S * sign(\dot{x})$$
$$-S_{K4}(\theta_S - \theta_3) - S_{K5}(\theta_S - \theta_4) \qquad (31)$$

S_{K4}, S_{K5} are, respectively, the torsional stiffness of the spine between suspension - lashing 3 and suspension – lashing 4.

4.4. Lashing spars

The equation of motion of the masses m_i placed at the lashing spars are (Fig. 8):

$$m_i * \ddot{x} = R_{Zi} - (F_{LZi} + F_{RZi}) \qquad (32)$$

$$m_i * \ddot{y} = R_{Yi} - (F_{LYi} + F_{RYi}) \qquad (33)$$

$$I_i * \ddot{\theta}_i = F_{RYi}[Z_{Ri}\cos\theta_i - B_{Ri}\sin\theta_i] +$$
$$+F_{LZi}[-Z_{Li}\sin\theta_i + B_{Li}\cos\theta_i] -$$
$$-F_{RZi}[Z_{Ri}\sin\theta_i + B_{Ri}\cos\theta_i] -$$
$$-F_{LYi}[Z_{Li}\cos\theta_i + B_{Li}\sin\theta_i] -$$
$$-S_{Ki,i-1}(\theta_i - \theta_{i-1}) - S_{Ki,i+1}(\theta_i - \theta_{i+1}) \qquad (34)$$

where S_{Ki-1} is the torsional stiffness of the spine between the mass i and the mass i-1.

We made the hypothesis that the motion of the trailer cannot affect ship motion because of the huge difference in their masses. Moreover, we assumed that the deck is completely rigid (this latter assumption is worthy of further investigation). The motion equations were programmed with *Mathematica* [18].

5. APPLICATION

5.1. Ship characteristics

The components of the roll equation (15) have been calculated for an existing Ro –Ro ship [14-15]. For the calculation of the equivalent damping factor B_e, we used the well-known method of Ikeda [16]. Figs. 10 and 11 show the GZ curve and the equivalent damping coefficient, whereas Fig. 12 shows the time history of the roll angle for $H/\lambda = 1/20$ and assuming resonant rolling. Fig. 13 shows the calculated roll angles at steady state for various H/λ, scaled with the angle of vanishing stability φ_v. The characteristics of the ship are shown below in Table 4.

Table 4

Ship characteristics			
L(m)	142	ùï (rad/sec)	0.479
B(m)	22.8	Öv(rad)	1.064
T(m)	6.4	Deck A (m)	6.4
Ä(tons)	11354	Deck B (m)	11.8
GM(m)	1.879	Deck C (m)	17.2
C_B	0.548		
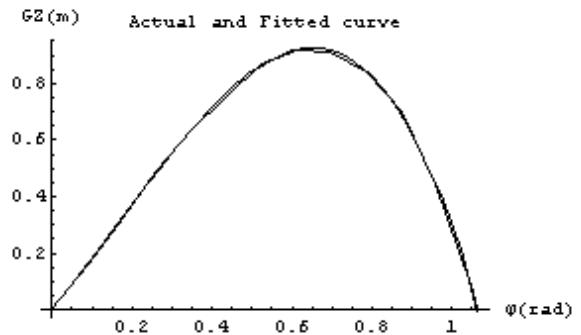
Fig. 10: The restoring curve of the examined ship.

118

*8th International Conference on
the Stability of Ships and Ocean Vehicles
Escuela Técnica Superior de Ingenieros Navales*
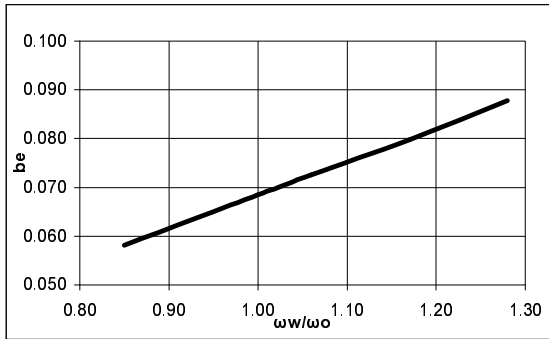

Fig. 11: The equivalent damping coefficient $b_e = B_e /(I + \delta I)$ as function of the frequency ratio.
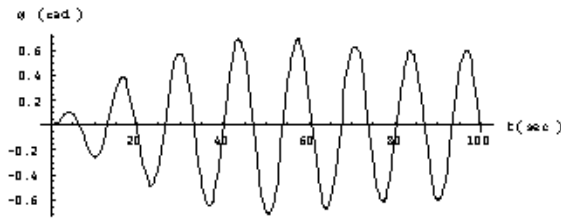

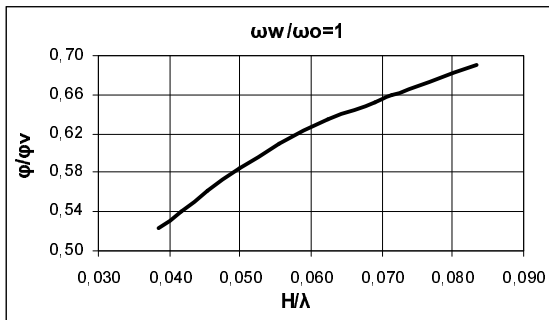Fig. 12: Simulated roll angle for $H / \lambda = 1/20$ and resonant rolling.

Fig. 13: Roll angles for increasing H/λ, assuming resonance condition.

5.2. Simulation results

We have examined the effect of various parameters classified in two categories: The first refers to the characteristics of the trailer and the lashing system, such as lashing stiffness and trailer's position. The second category refers to the sea environment taking into consideration wave steepness and wave frequency.

Trailer – lashing system:

Firstly, we determined the lashing loads for the reference parameter values given in Table 5. In this condition the trailer lies exactly at the roll axis, so $r = 0$ (see Fig. 9). In Fig. 14 is shown the time history of the lashing force 2, while Fig. 15 summarises the maximum loads at the lashings attached to the spars for $H / \lambda = 1/20$ and $\lambda/B = 11.75$. It can be observed that the maximum load appears at position 2.
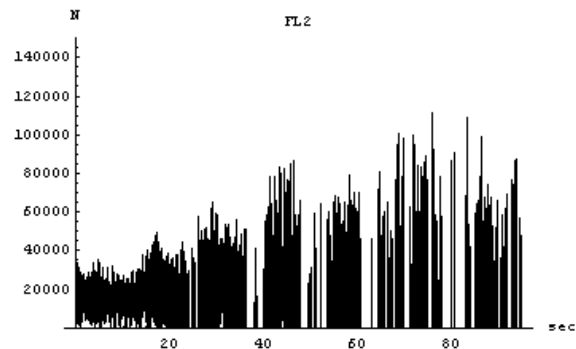

Fig. 14: Time history of the left lashing load 2.

The effect of stiffness of the lashing at position 2 on the experienced load is shown in Fig. 16.

Another parameter examined was the position of the trailer. The Ro/Ro ship on which we based our calculations had three vehicle decks. The trailer could be placed on the centreline of the ship or at a distance b sideways. The values b can range from 0 to $B/2$, where B is the breadth of the ship. Fig. 17 shows the results of the simulations for the vertical and transverse position of the trailer with respect to the loads for lashing 2.

Finally we examined a special case, in which the left lashing 3 was not properly connected with the spine and as a result it had no load

8th International Conference on
the Stability of Ships and Ocean Vehicles
Escuela Técnica Superior de Ingenieros Navales

119

bearing capability. In Fig. 18 can be seen the loads developed on the remaining lashings in comparison with the loads that correspond to the standard condition. It is apparent that failure to attach properly one or more lashing can lead to excessive loads on the others which can be well above their MSL values.

Table 5

Trailer – lashings characteristics			
A_L, A_R (m)	1.5	λ (KN*s/m)	15
B_S, B_T (m)	0.9	X_S (m)	10.5
B_L, B_R	0.9	X_{Li} (m)	1, 2, 4.5, 2,1
m_5, m_6 (tons)	10	Z_G (m)	0.85
m_i (tons), i=1,…4	2.5	Z_S (m)	0.85
I_5, I_6 (tons*m^2)	5	Z_T (m)	1
I_i (tons*m^2) i=1,…,4	1.25	Z_{SS} (m)	0.15
K_T (MN*m)	40	Z_{TS} (m)	0
K_S (MN*m)	1	Z_{Li}, Z_{Ri} (m)	0.15
K_{Li} (MN/m/m)	8	μ_T	0.3
S_K (MN*m/rad)	1.5	μ_S	0.5
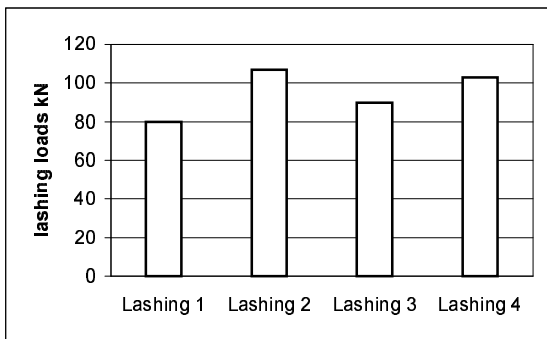
Fig. 15: Maximum loads on each lashing for the parameter values shown in Table 5.
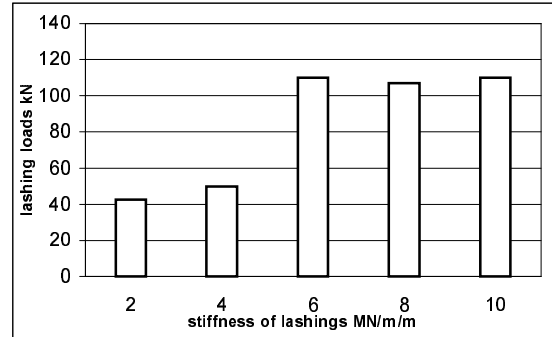
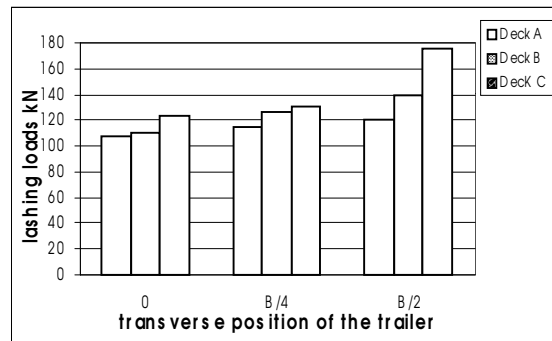Fig. 16: Maximum load for lashing 2 as function of its stiffness.

Fig. 17: Variation of lashing load at position 2 depending on the vertical and transverse position of the trailer on the ship.
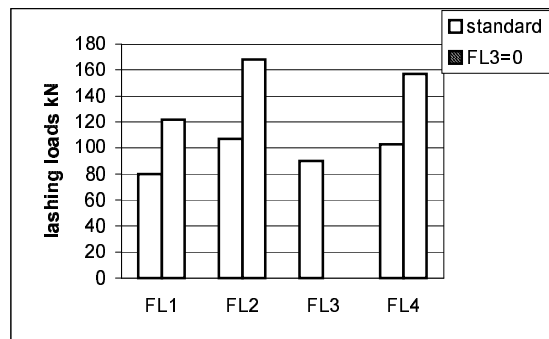

Fig. 18: Maximum loads when the left lashing 3 is not connected with the spine.

The sea environment

We ran simulations for various values of wave steepness while keeping constant the ratio of wave frequency to roll's natural

120

*8th International Conference on
the Stability of Ships and Ocean Vehicles
Escuela Técnica Superior de Ingenieros Navales*

frequency ω_w / ω_o. In Fig. 19 are shown the obtained loads on the lashings at position 2. As expected, the load is increasing with the wave steepness and in fact the relation is essentially linear.

The effect of wave frequency on lashing loads for fixed wave steepness $H / \lambda = 1/20$ is shown in Fig. 20. Due to the nonlinear effect the maximum rolling occurs to the left of the frequency ratio of linear resonance and this trend is reflected also on the magnitude of lashing loads.
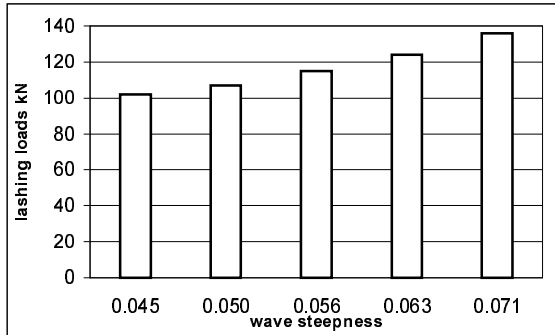
Figure 19: Variation of loads on lashing 2 with wave steepness.
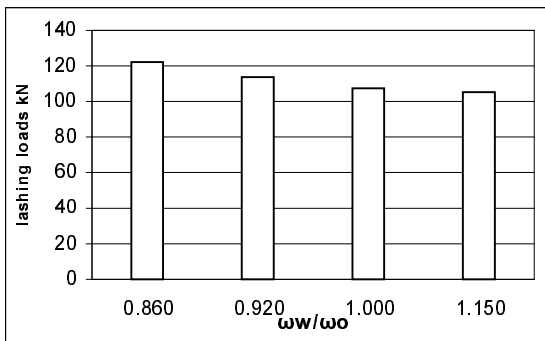
Fig. 20: Variation of the lashing load at position 2 as function of the frequency ratio

6. FINITE ELEMENT ANALYSIS

In this section, we are coupling the analysis of trailer motion dynamics with an analysis of strength based on a finite elements approach. In the examples discussed below we have concentrated on the strength at the point where the lashing is attached to the trailer. In terms of strength this is a critical location of the securing device. Such links can have various shapes and in Fig 21 is shown a possible geometry. For the calculation of the stresses we carried out a finite element analysis based on the commercial code *ALGOR* [19]. Scenarios featuring both static and dynamic loadings of the link were considered and the corresponding distributions of stresses were determined. The assumed loading is the maximum lashing force and is obtained with the simulations of the previous section.

We developed also a model for the situation where the lashing, while being initially slack, is subjected to instantaneous loading. This is near to an impulsive loading case and it is expected to represent a critical condition in terms of strength.

6.1. Geometry of the link

Fig. 22 shows a side view of the lashing system, which includes the lashing and the link. We assumed that the link has been welded to the body of the trailer. The type and dimensions of the chain link were determined after searching in catalogues for chains. The geometry finally used in our modelling is presented in Fig 23.
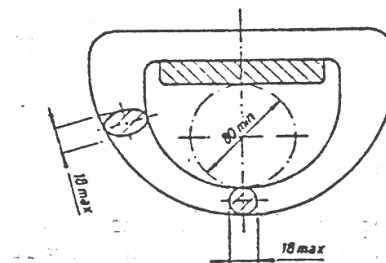

Fig. 21: A typical shape of the connection point of the lashing on the trailer.

8th International Conference on
the Stability of Ships and Ocean Vehicles
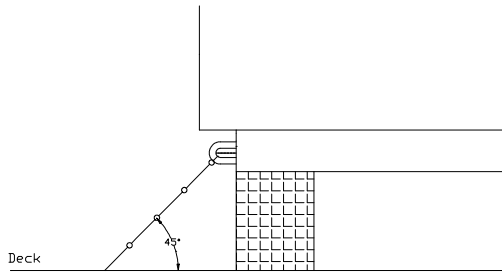*Escuela Técnica Superior de Ingenieros Navales*

121

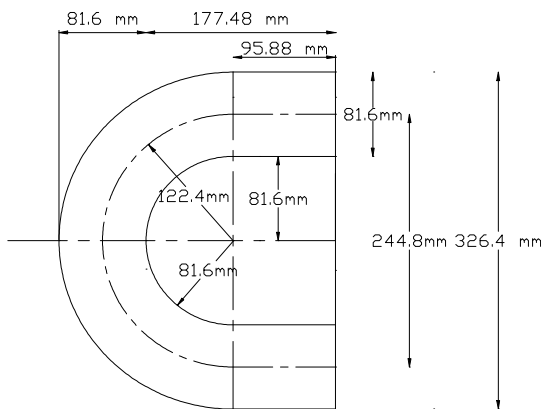Fig. 22: Transverse section of trailer and securing device. The securing angle is 45°.

Fig. 23: The studless end link. The proof load for pure tension is 1230 Kn.

6.2. Static and Dynamic Analysis

The complete modelling process with the program ALGOR is detailed in [15]. Fig. 24 shows how the link was split in beam elements. Furthermore, Fig. 25 shows the direction of the force and the connection points between the link and the trailer. The link is firmly attached to the trailer. Axis x is parallel to the deck and is vertical to the axis of the trailer. The static loading condition is determined as follows:
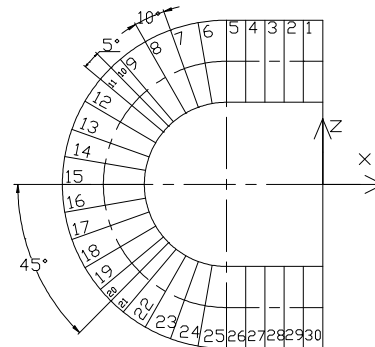

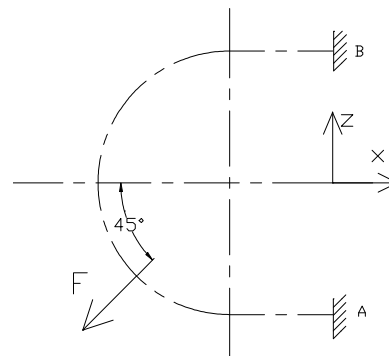Fig. 24: The beam elements of the link.

Fig. 25: The centre line of the cross section.

From the results of the simulation the maximum lashing load was experienced at lashing 2 when the trailer was placed on Deck C and its transverse distance from the centreline was B/2 (see also Fig. 26). For the static analysis, we examined the following three cases:
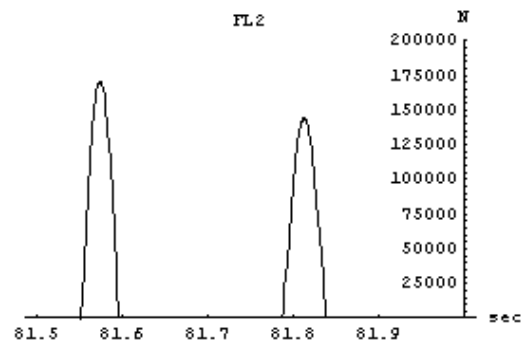

Fig. 26: Load on lashing 2 as function of time (max F=176kN)

*8th International Conference on
the Stability of Ships and Ocean Vehicles
Escuela Técnica Superior de Ingenieros Navales*

122

a. According to Fig. 25, the static force has direction that forms an angle of 45° with the axis *x* and magnitude 176 kN.

b. The same as case (a), but the static force forms an angle of 5° with the plane *xz* (Fig. 25). This out-of-plane loading corresponds to the case where the lashing is not in the same plane with the link because of a small longitudinal movement of the trailer.

c. The same as case (b), but the angle out of plane is 10°.

Using the *Linear Static Stress Model* of ALGOR, the distribution of stresses and the displacements were determined for the edge of the cross section of the link. This is where the maximum values arose. The total stress is the algebraic sum of the stresses due to bending and tension. Fig. 27 shows a typical result for the distribution of stresses.

The results for these static cases are summarised in Fig. 28 and 29. We assumed that the material of the link is steel and the maximum stress load is 245 Mpa.
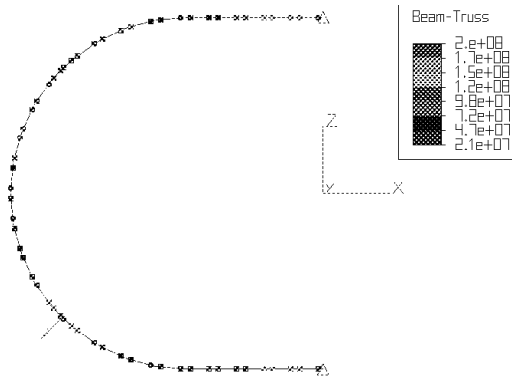

Fig. 27: Distribution of stresses for the third static situation.
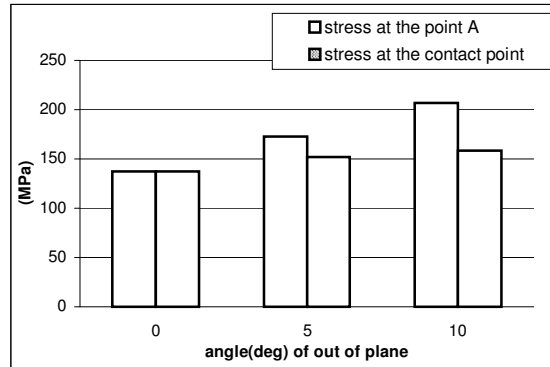

Fig. 28: Maximum stresses at point A for the three static cases and at the point of contact where the maximum stresses were found.
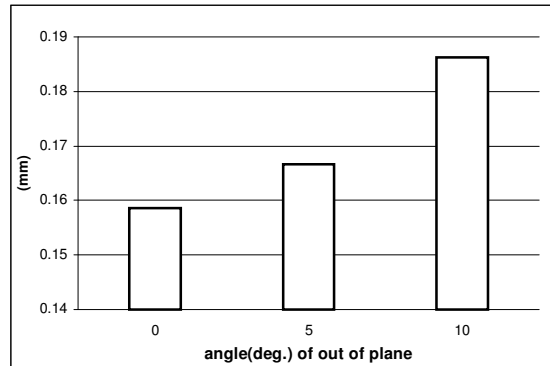

Fig. 29: The maximum displacements (at the point of contact) for the three static cases.

From Fig. 28 and 29, we can notice that when there is an angle out of plain, the same loading leads to higher stresses at the link.

In the 'dynamic' scenario we have considered time-varying loading of the link as shown in Fig. 30. This analysis of dynamic loads was carried out with ALGOR's *Linear Transient Series* module.

8th International Conference on
the Stability of Ships and Ocean Vehicles
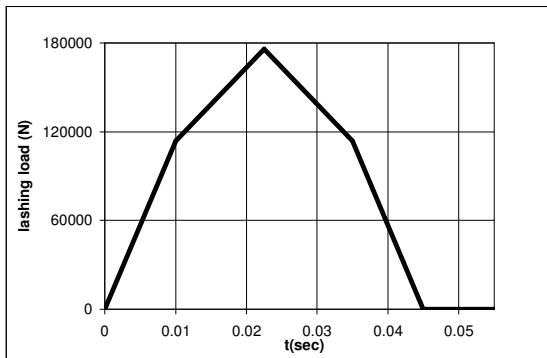*Escuela Técnica Superior de Ingenieros Navales*

123

Fig. 30: Assumed time variation of loading for lashing 2.

The time considered was 0.055s and we have used 50 time steps. However the lashing load was applied for a fraction of this time (0.045s). The geometry shown in Fig. 25 is still valid for the direction of the force and there is no angle out of plane. The model calculates the distribution of stresses and the displacements at every time step. For the point A and the contact point the time history of the stresses is shown in Fig. 31
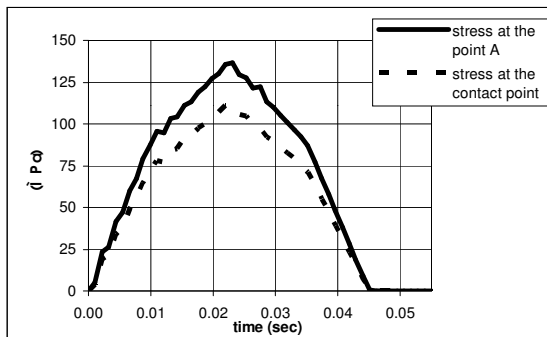

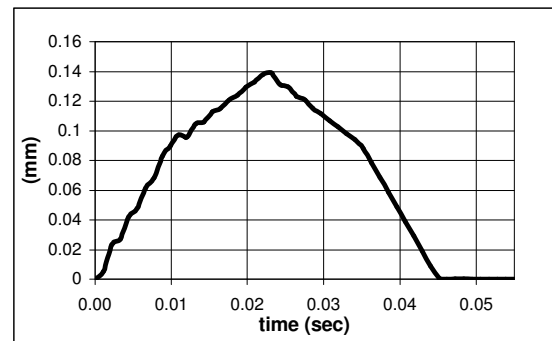Fig. 31: Stress time history for the dynamic load.

Fig. 32: Time history of the displacement at the contact point in the dynamic loading case.

The time history of displacement at the contact point is shown in Fig 32. Comparing Figs. 28, and 31 with Figs. 29 and 32 we notice that the maximum values of stresses and displacements for the dynamic loading condition are comparable to the static ones. This result from the fact that the dynamic loading cannot be considered as impact loading since the change of the load in time was quite "slow".

6.3.   Strength   analysis   due   to   the impulsive loading of the lashings.

Perhaps the most interesting condition arises when the lashing is slack and then it is loaded suddenly up to a maximum value. This loading can be taken as impulsive. In this subsection, we shall build a model to estimate the stresses that arise at the link. In the models that we used in the previous sections we considered that the lashings are always under tension i.e. they could not be slack. However, if a lashing is slack, this should allow trailer motion until the lashing is loaded. For this analysis we used the *Mechanical Event Simulation* module of ALGOR (with nonlinear material models). The complete analysis can be found in [15]. The basic steps of this approach and some results are as follows:

We assumed that the trailer moves 5cm in the transverse direction due to slackening of the

124

*8th International Conference on
the Stability of Ships and Ocean Vehicles
Escuela Técnica Superior de Ingenieros Navales*

lashings until this motion is stopped. We have modelled the lashing as a truss element, whereas the trailer as a beam element. The link is modelled again as a set of beam elements. As there are four lashings, the mass of the trailer is split into four equal parts. Fig. 33 shows this modelling.
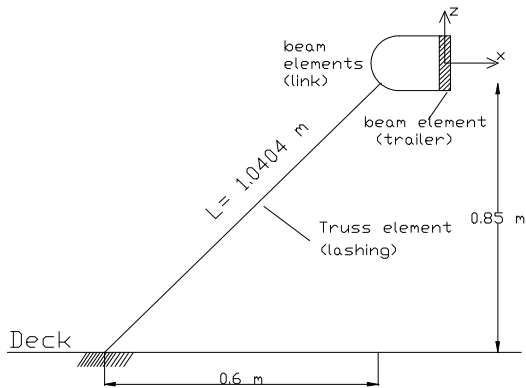

Fig. 33: The modelling of the system lashing–link– trailer. The dimensions are according to Table 5.

The next step is to determine the acceleration of the trailer due to the maximum lashing load, assumed to be 176 kN. We must underline that because the transverse trailer motion is sustained from the transverse component of the lashing force, the value of 176 kN keeps us on the safe side. Thereafter we calculate the velocity of the trailer when it has moved by a distance of 5 cm and also the natural frequency of the system according to the stiffness of the lashing and the mass. Knowing the total time of the motion of the system, the model calculates for a number of time steps the distribution of stresses and the displacement of the link.

The simulation of the system's motion is carried out as follows: firstly, the trailer will move to the positive side of the *x* axis according to Fig. 33. When the system reaches the position of maximum movement, it will

begin to return back towards its initial position. The distribution of the stresses at the time step when the distance from the initial position is maximum is shown in Fig.34.
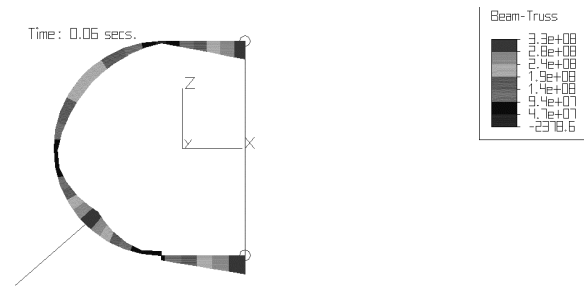

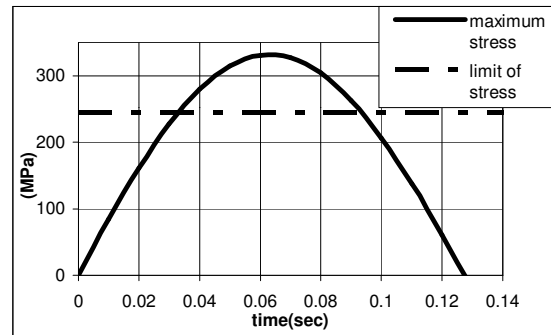Fig. 34:   Distribution of stresses at the time step of maximum movement.

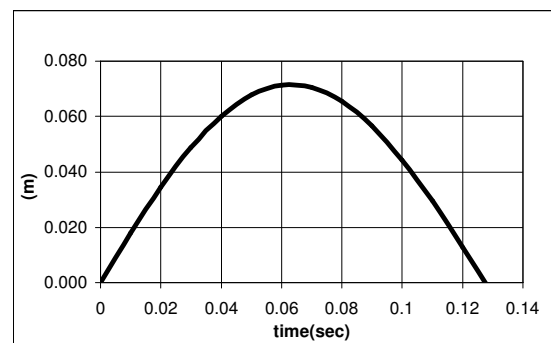
Fig. 35: Time history of the maximum stress

Fig. 36: Time history of the motion of the system

8th International Conference on
the Stability of Ships and Ocean Vehicles
Escuela Técnica Superior de Ingenieros Navales

125

Fig. 35 shows the time history of the stresses for the points where the lashing is attached to the link and for the points where the link is connected with the trailer. At these points the stresses have their maximum values. From Fig. 35, we notice that the stresses are quite larger than the limiting stress. Fig. 36 shows the time history of the motion of the system.

7. CONCLUDING REMARKS

We have developed an integrated approach for assessing the adequacy of lashing systems on board RO-RO ferries, taking into account ship and trailer dynamics and detailed strength analysis at the links.

Our simulation results show that the experienced lashing loads may be different from those predicted according to the CSM calculation method. This comes from the fact that our modelling of the trailer takes into account the trestle and suspension as well as the torsional flexibility of its spine.

IMO require for the lashings to have a minimum strength, without permanent deformation, of 120kN. In some examined cases loads higher than this limiting value were found. The loads are sensitive to several factors: The increase of lashing stiffness results in increase of lashing loads up to a limit (Fig.16). As expected, the position of the trailer proved to be of critical importance for the loads (Fig. 17). Thus heavy trailers should be stowed on the lower decks and near to centerline. The crew responsible for securing the trailers on board should perform their duty meticulously because inappropriate securing of even one lashing could lead to serious increase of the loads on the other lashings (Fig. 18). The sea environment affects straightly the rolling motion of the ship and the lashings loads as Figs. 19 and 20 show.

Our strength analysis revealed that the angle out of plain (Fig. 28) plays a major role for the level of stresses at the link of the lashing with the trailer. A slack lashing could bring about significantly higher stresses due to impulsive loading as compared to the smooth loading case (Fig. 35). This is another reason why a proper inspection of the securing system before and during the journey is of primary importance.

Finally we should underline that the model presented in this paper is not complete and it needs further expansion in order to include also other important motions of the ship; especially the pitch, and also the excitation in an irregular sea.

8. ACKNOWLEDGMENT

9. NOMENCLATURE

9.1. Ship characteristics:

B :   breadth

B_e :   equivalent damping factor

D_C ,

D_B , : height of decks C, B and A

D_A

GM : metacentic height

$I, \delta I$: moment and added moment of
        inertia in roll

L :   length

T :   draught

Δ :   displacement

φ :   roll angle

φ_v :   angle of vanishing stability in roll

ω_o :   natural roll frequency

*8th International Conference on
the Stability of Ships and Ocean Vehicles
Escuela Técnica Superior de Ingenieros Navales*

126

9.2. Sea characteristics:

H :   wave height
λ :   wave length
ω_w :   wave frequency

9.3. Trailer and lashings characteristics:

A_L, A_R : left and right distances
between the lashings points on the deck and the spine

B_S, B_T : half width of the chassis at the suspension and trestle

B_L, B_R : left and right width of the chassis at the lashing spars

I_5, I_6, I_i : moments of inertia of each mass about its centre

K_T, K_S : stiffness of the springs of the trestle and suspension

K_{Li} :   stiffness of left and right hand lashing i

L, L_0 :   instantaneous and initial lashing lengths

m_i :   lumped mass at position i

S_K :   torsional stiffness of a unit length of spine

X_S :   total length of spine

X_{Li} :   distances between the masses

Z_G :   height of the masses above the spine

Z_S :   height of the suspension after loading

Z_{SS} :   vertical distance between the top of suspension and the spine

Z_T :   height of the trestle after loading.

Z_{TS} :   vertical distance between the top of the trestle and the spine

Z_{Li}, Z_{Ri} : vertical distance between the $\underline{i}^{\text{th}}$ spar and the spine

λ :   damping constant of the suspension

μ_T :   friction coefficient between the trestle and the trailer

μ_S :   friction coefficient between the suspension and the deck

10. REFERENCES

[1]   IMO (1981) *Safe stowage and securing of cargo units and other entities in ships other than cellular containerships*. Resolution A. 489.

[2]   IMO (1983) *Elements to be taken into account when considering the safe stowage and securing of cargo units and vehicles in ships*. Resolution A.533.

[3]   IMO (1984) *Guidelines for securing arrangements for the transport of road vehicles on Ro – Ro Ships. Resolution* A.581.

[4]   IMO (1985) *Containers and cargoes (BC) cargo securing manual*. MSC/Circ. 385.

[5]   IMO (1991) *Code of safe practice for cargo stowage and securing and amendments thereto*. Resolution A.714 (with 1994/95 amendments, Annex 1-13).

[6]   IMO (1996) *Guidelines for the preparation of the cargo securing manual*. MSC/Circ. 745.

[7] ISO (1989)   *Lashing and securing arrangements on road vehicles for sea transportation on Ro/Ro ships - General requirements - Part 1: Commercial vehicles and combinations of vehicles, semi-trailers excluded*. 9367-1:1989.

[8]   ISO (1994) *Lashing and securing arrangements on road vehicles for sea transportation on Ro/Ro ships - General requirements - Part 2: Semi-trailers*. 9367-2:1994

[9]   U.K. Department of Transport, Marine Directorate (1991). *Roll-on/roll-off ships:*

8ᵗʰ International Conference on
the Stability of Ships and Ocean Vehicles
Escuela Técnica Superior de Ingenieros Navales

127

stowage and securing of vehicles-code of practice, ISBN 011 550995 X.

[10] Det Norske Veritas (2002) *Cargo securing manual: model manual*. Version 3.1.

[11] Andersson, P. (1984) *Securing of road trailers on board RO/RO ships*. Mariterm AB, IMO Conference, London.

[12] Turnbull, S.R. & Dawson, D. (1994) The securing of vehicles on roll – On/roll – off ships. RINA *Transactions*, **135**, 37-51.

[13] Turnbull, S.R. & Dawson, D. (1999) The dynamic behaviour of flexible semi-trailers on board RO-RO ships. *International Journal of Mechanical Sciences*, **41**, 1447-1460.

[14] Papagiannopoulos S. (2001) *Investigation of ship capsize in beam seas based on nonlinear dynamics theory*. Diploma Thesis. National Technical University of Athens, School of Naval Architecture and Marine Engineering.

[15] Themelis N. (2002) The securing of trailers on the vehicle deck of a Ro-Ro ship under intensive rolling. Diploma thesis. National Technical University of Athens, School of Naval Architecture and Marine Engineering.

[16] Himeno, Y. (1982) Prediction of ship roll damping – state of the art. Report, dept. of Nav. Arch. And Mar. Engn., The University of Michigan.

[17] Bhattacharyya. R., (1978) Dynamics of Marine Vehicles, John Wiley & Sons, Chichester.

[18] The Mathematica Book, version 4.0 (2001), Wolfram Media Inc. ISBN 1-57955-004-5.

[19] Algor Release Notes and Reference Manual (2001), ALGOR-Inc.